ARMA 16-0150

Well stimulation in tight formations: a dynamic approach

Omidi, O. and Abedi, R.
Department of Mechanical, Aerospace & Biomedical Engineering, The University of Tennessee Space Institute, TN, USA

Enayatpour, S.
Center for Petroleum and Geosystems Engineering, The University of Texas at Austin, TX, USA

ABSTRACT: Hydraulic fracturing is widely employed for well stimulation. Different techniques have been utilized in practice to optimize fracking in the last five decades. However, it has some disadvantages including a lack of control over the direction of fracture propagation, the high treatment cost along with environmental issues. Producing multiple fractures by dynamic stimulation techniques seems to be more promising in naturally fractured reservoirs, since it is an effective way for connecting a pre-existing fracture network to a wellbore. In this study, applying high rate loadings we investigate fracturing in rocks due to explosives and propellants as two common methods for dynamic stimulation of a well. An interfacial damage model implemented in a Spacetime Discontinuous Galerkin finite element framework is utilized to simulate fracturing in rocks. A powerful dynamic mesh adaptivity scheme is implemented to track arbitrary crack paths and align them with element boundaries. High explosives produce shockwaves causing extreme compressive stresses, which results in crushing and compacting the rock around the wellbore. Propellants can generate a pressure pulse producing a fracturing behavior that loads the rock in tension. The main advantage of this later approach is to create multiple fractures and consequently prepare the well for an effective hydraulic fracturing with much lower cost as a re-fracturing solution.

Acknowledgments: The authors gratefully acknowledge partial support for this study via the U.S. National Science Foundation (NSF), CMMI - Mechanics of Materials and Structures (MoMS) program grant number 1538332.

1 INTRODUCTION

Stimulation treatments to enhance hydrocarbon recovery from shale and other tight formations as unconventional resources are mainly classified into fracturing based on hydraulic, thermal and dynamic loadings. There is no alternative to fracturing itself, since it is the only way to artificially fissure the source rock to provide sufficient permeability for oil and gas extraction cost-effectively. The technology of hydraulic fracturing which is also called fracking has been widely employed since 1949. It has been very common and popular in oil industry for decades owing to technological advances in practice. Horizontal drilling was a complement to this method since the late 1980. This technique was developed further in 1997 by the use of chemicals known as slickwater fracturing in which slickwater is water mixed with friction-reducing additives. Employing these advances along with the development of multi-well pads have made gas production from shales technically and economically feasible especially in North America in the last decade.

However, hydraulic fracturing has been a controversial topic as an environmental concern during development of gas shale reservoirs located near populated residential regions. Due to the use of water in the fracking technique, one of the main worries is its potential impacts on environment including the danger of possible contamination of groundwater. This issue certainly depends on the complexity, scale and frequency of the hydraulic fracturing required for an area. The conventional hydraulic fracturing methods usually produce a few number of main hydraulic cracks interacting with natural fissures. Huang *et al.* in 2011 showed that using water blasting for fracturing coal seams can enhance the effectiveness of hydraulic fracturing by increasing the number and range of cracks resulting in an improved permeability [1]. In this technique, water pressure blasting is carried out

by detonating the gel explosive located in a drilled well. The shock waves generated by the explosion cause a high strain rate in the rock wall surrounding the hole. The rock breaks and numerous circumferential and radial fractures propagate outward. A conventional hydraulic fracturing is subsequently performed as the final stage so that the fissures open by the detonation are further develop and propagate. Reducing the quantity of water required for the hydraulic fracturing stage, this method is potentially applicable to the formations having low permeability. As noted above, there exist other methods for the formation stimulation that are not water-based. For instance, dynamic fracturing by either explosive, electric discharge or propellant and the methods utilizing fluids or chemical materials other than water.

Different numerical methods have been employed for the hydraulic fracturing simulations. These numerical approaches are conventionally categorized into discrete and continuum methods to address fracturing in such a naturally fissured material. The category of discrete approaches include peridynamics and particles methods. Developing a continuum plastic–damage model, Shojaei *et al.* simulated the hydraulic fracture propagation with the effect of injected pore pressure in the developed fracture surfaces [2]. Using a proposed elastic–plastic damage model for rock and a dynamic solution technique, Busetti *et al.* studied the effect of far-field stresses and pressure distribution in the fracture on the geometric complexity of the fractured regions [3]. Furthermore, as a granular material, fracturing in tight formations can be modeled by the discrete element method [4, 5]. The *extended finite element method* (XFEM) and the *generalized finite element method* (GFEM) representing the crack faces by enriching the solution space with discontinuous functions has been widely used for the hydraulic fracture problems [6–8]. Dahi-Taleghani and Olson used the XFEM in a 2-D implementation and addressed the interaction between the induced hydraulic fracture and natural fractures/weak planes in these naturally fractured formations [6].

Including the fluid pressure degrees of freedom in the formulation, Chen *et al.* proposed a simultaneous solution for the fully coupled fluid flow and resulting crack propagation by a special XFEM implementation [7]. Besides, Mohammadnejad and Khoei employed the XFEM for hydraulic fracture propagation by developing a coupled numerical tool [8]. Focusing on propagating fractures with complex geometries, like those encountered in early stages of hydraulic fracturing, Gupta and Duarte proposed a GFEM for the simulation of non-planar 3D hydraulic fractures [9]. In their proposed GFEM, the representation of fracture surfaces is independent of the volume FE mesh and consequently, complex surface features like sharp turns and kinks can be accurately captured. Later on, Gupta and Duarte further developed their implementation by presenting a coupled hydromechanical GFEM formulation for the simulation of non-planar three-dimensional hydraulic fractures [10]. Gordeliy and Peirce proposed a coupled algorithm using XFEM to solve the elastic crack component of hydrodynamic equations governing the propagation of hydraulic fractures in an elastic medium [11]. Bazant and Caner proposed dynamic fracturing based on the kinetic energy of high-rate shearing generated by an underground explosion to reduce the rock to small fragments [12]. Using arc pulse electric discharge method, Chen *et al.* computationally and experimentally examined how this technique can improve permeability of concrete [13].

Although the XFEM techniques in which remeshing is unnecessary have been developed to model cracks independently of the FEM mesh [14], including rock mass discontinuities is problematic in XFEM-based simulations. On other hands, the *discrete element methods* (DEMs) have been widely used to overcome this limitation of continuum models [15]. In DEM, rock mass discontinuities can be explicitly simulated along with fluid flow in the fracture network. However, since position and geometry of fractures must be assumed a priori, initiation and growth mechanisms cannot be implicitly embedded for a probabilistic nucleation in DEM.

Employing the *Spacetime Discontinuous Galerkin* (SDG) finite element method formulated for elastodynamics for our analysis, we discuss an alternative approach to simulate dynamic fracturing based on explosive and propellant techniques for stimulation of tight formations. The key feature of the SDG method is direct discretization of spacetime using unstructured grids that satisfies a special causality condition. This yields a local and asynchronous solution strategy with linear computational cost scaling vs. number of elements [16]. It also enables arbitrarily high orders of accuracy both in space and time per element. These features, which are otherwise difficult to achieve with conventional time marching schemes, result in a very accurate and efficient numerical method. Of particular importance to hydraulic fracturing, it is the ability of the method to align inter-element boundaries with user-specified interfaces in spacetime. This technique well captures modes I and II of intact material breakage as well as shearing along newly created and pre-existing fractures.

The other features this SDG can possibly address are fracture branching and coalescence, material heterogeneity along with rock mass discontinuities. Adaptive meshing allows propagation of cracks in the domain based on crack-path trajectories that are obtained as a part of the solution according to a crack growth criterion. Thus, this model does not suffer the mesh-dependent effects encountered in most other numerical fracture models. There are several distinct differences between our approach and the XFEM/GFEM methods. First by dynamically adjusting the mesh in spacetime, we align the element boundaries with predicted crack paths; unlike the XFEM methods no special discontinuity functions are required. Second, complicated crack pattern scenarios such as microcracking and crack bifurcation do not pose additional challenges in our approach, as again no enrichment functions are needed to model them within the elements. Finally, since the elements are not enriched with crack field functions, no special quadrature rules are required for their integration [17].

2 FORMULATION

2.1 Overview of the SDG method

Discontinuous Galerkin (DG) techniques are a special class of finite element methods in which discontinuous basis functions are used for elements. Continuity between elements is enforced a priori in *continuous finite element methods* (CFEMs), while this condition is weakly imposed via the jumps between elements in DG methods. Although they have more average degrees of freedom per element, there are two distinct advantages over CFEMs in a transient analysis. First, in DG methods mass matrix has a block diagonal form resulting in a linear solution cost scaling versus number of elements. This is achievable in CFEMs only by the so-called mass lumping which can adversely affect the convergence rate in the problems where higher orders of accuracy are important and desirable. Second, due to their discrete solution space and treatment of fluxes between elements, DG methods typically perform much better for problems tending to either preserve discontinuities and shocks in initial and boundary conditions or create them if nonlinearities are present. Consequently, they do not suffer from global nonphysical oscillations, a feature commonly observed with CFEMs.

2.2 Adaptive schemes for dynamic fracturing in rocks

2.2.1 Mesh adaptive operations

The most practical time discretization procedures employ either *implicit* or *explicit* operators to advance the solution in time. Herein, instead of using a time integration scheme, as illustrated in 1(a) for a simple $1d\times$time causal mesh we directly discretize the spacetime using unstructured grids that satisfy a special causality constraint enabling us to utilize local solutions for small collections of connected elements. High temporal orders of accuracy and adjusting them per element are distinct features of direct discretization of spacetime with finite elements. Both aspects are particularly challenging within the framework of methods that employ a time marching scheme, distinct from spatial finite element, to advance the solution in time. Moreover, the asynchronous structure of the SDG method has very important implications for multiscale simulations and parallel computing. Explicit time marching methods are often more efficient but suffer from very restrictive time steps for spatial meshes with vastly different element sizes. While hybrid *implicit-explicit* (IMEX) and *local time stepping* (LTS) alleviate this problem to some extend, the time advance for distinct spatial element sizes are completely decoupled in the SDG method resulting in a very efficient scheme for multiscale grids. Besides, in parallel computing, usual time marching (Figure 1(b)) results in global synchronization which can be a limitation in parallel efficiency. The asynchronous structure of the SDG method directly addresses this issue. The causal SDG meshes enable asynchronous, element-by-element solutions with linear complexity [16, 18].

The SDG method's features discussed above are of particular importance to dynamic fracturing in rocks. First, high gradient mechanical solutions around moving crack tips require high order and stable numerical methods. Second, to resolve fracture process zone with high fidelity and maintain an efficient solution scheme, a very small ratio of the elements around the crack tip to the largest elements in the domain results in highly multiscale grids. Thus, a spatially and temporally high order numerical method such as the SDG method that can efficiently simulate multigrid meshes is of immense importance. Another level of complexity arises from moving wave fronts and evolving crack paths in dynamic fracture problems. The interested readers are referred to [17, 19] for the general analysis of the SDG method, and [20, 21] for adaptive features pertained to elastodynamics and fracture mechanics.

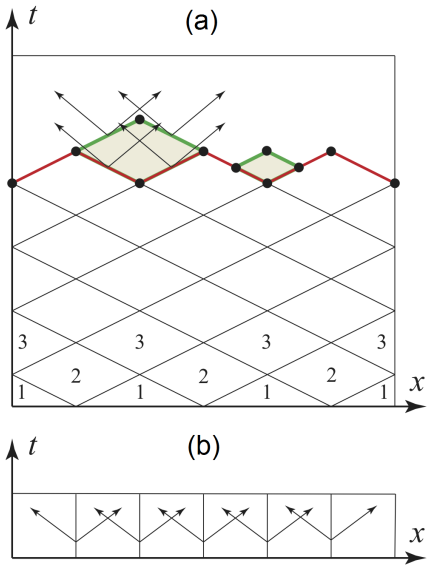

Figure 1: SDG Solution scheme on causal spacetime mesh in $1d\times$time (top). Global coupling in non-causal mesh (bottom). Reproduced from [18]

2.2.2 Crack path tracking strategy

There are different crack path tracking strategies available in finite element methods including continuum buck damage models, discrete cracking by either fixed or adaptive meshes and the XFEM-based simulations. Continuum damage models do not capture physical fracture faces and cracks are represented only as smeared regions in the bulk with a localized path. Furthermore, utilizing a fixed discretization, crack propagation is restricted to existing element boundaries. Obviously, handling mixed mode loadings in which the crack path is not predictable is challenging and the predicted crack path is not reliable in simulations using fixed meshes.

On the other hand, adaptive meshing scheme is a suitable approach for modeling crack propagation because element boundaries are aligned with predicted crack paths. However, simulating crack growth using the classical FEM is quite difficult because the topology of the domain changes continuously. On the other hand, allowing to simulate arbitrary discontinuity with a fixed mesh, the XFEM method follows a crack path within the elements and the domain does not need to be re-meshed as the crack propagates. Although the XFEM alleviates the problem of modeling arbitrary cracks and discontinuities of the finite element mesh, incorporation of nonlinear mechanisms such as damage and plasticity at the crack interface is still a challenge in the available XFEM implementations. Furthermore, different crack pattern topologies, such as microcracking and bifurcation, demand the derivation and inclusion of additional enrichment functions. Our approach to model complex fracture patterns fall into adaptive meshing category discussed above.

2.2.3 Probabilistic nucleation

Stochastic distribution of natural fractures and pre-existing crack-like defects plays a critical role in fracture process of rocks. Cracks initiated from these defects are often accelerated through increasing stress concentrations induced by initial fracture growth and local inhomogeneity. Energy absorption and stress release due to these local features of fracturing process result in a very non-uniform failure pattern at mesoscale. Since deterministic continuum models treat the material as perfectly homogeneous, they are capable of predicting simultaneous failures at regions of high stress, which is not physical. To address this issue at the continuum level, a probabilistic nucleation model can be devised where cracks nucleate from pre-existing fractures that are randomly distributed in rocks.

As discussed in the previous section, the SDG adaptive meshing scheme aligns the boundaries of spacetime elements with crack-path trajectories having arbitrary position and orientation. The cracks nucleation is based on a probabilistic model trying to simulate the nucleation process from randomly distributed pre-existing fractures which can be observed experimentally. Assuming a random distribution of material defects throughout the domain, the situation of individual defects varies according to the probability distribution. Let $\tilde{s}_N^j(x)$ denote the nucleation strength of a defect j in the mesoscopic neighborhood of a point x in the simulated area as illustrated in Figure 2. Let us assume that the number of defects in $N(x)$ is $n = \rho^{\mathrm{N}} A$ while ρ^{N} is the density of defects and A denotes the spatial measure of $N(x)$.

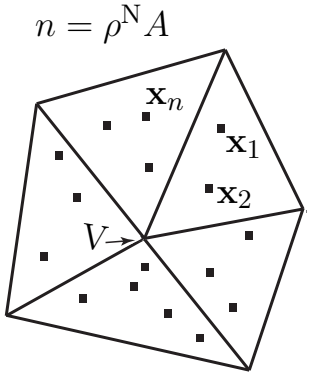

Figure 2: A possible distribution of defects as sampling points around a vertex

Assuming that the material's resistance to nucleation at any defect is isotropic, nucleation of a new fracture surface occurs at defect j when the maximum effective traction over all possible surface orientations at the defect, denoted by s^*, exceeds that defect's nucleation strength; *i.e.* when $s^* > \tilde{s}_N^j$. Therefore, having several sampling points in a specified region surrounding a vertex, we need to examine this criterion with $s^* > \tilde{s}_N^{min}$ in which $\tilde{s}_N^{min}$ is the minimum of nucleation strength among all possible sampling points as:

$$\tilde{s}_N^{min} = \text{Min}\{\tilde{s}_N^1, \tilde{s}_N^2, \tilde{s}_N^3, ..., \tilde{s}_N^n\} \tag{1}$$

The effective traction over the surface with angle θ shown in Figure 3 is defined as the following:

$$s_{eff}(\theta) = \sqrt{< s_n(\theta) >^2 + \beta^2 \ (s_t(\theta))^2} \tag{2}$$

where β is the shear stress factor controlling mode mixity; s_n and s_t are the normal and tangential components of traction acting on the interface in bonded mode. The positive-part operator ensures that only tensile stresses drive the damage evolution.

Similarly, an existing fracture surface will extend from its edges (endpoints in two dimensions), in a direction determined by the maximizing surface orientation, when $s^* > \tilde{s}_N^j$ for a defect j in the neighborhood of the edge.

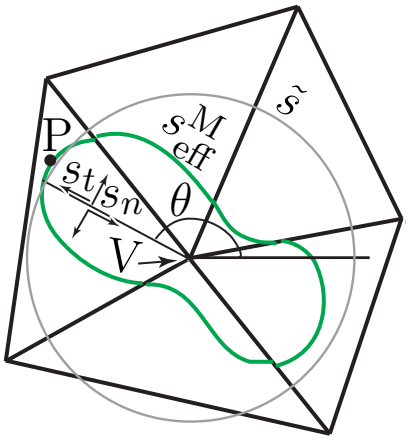

Figure 3: The circumferential distribution of effective stress and crack propagation criterion

When nucleation or extension is examined in our implementation, we generate a number of defect tests proportional to the volume of the element or region under consideration. For each defect test, we generate a randomized nucleation strength according to an assumed probability distribution. If any test indicates a positive result, then we implement nucleation or extension through the adaptive meshing capabilities of our spacetime code. The probability distribution is designed to ensure that nucleation and extension occur at effective traction levels somewhat lower than the damage threshold traction, $\underline{s}$. This ensures that the new fracture surface is in place, with damage initialized to zero, when the threshold traction is attained [17].

2.3 Interfacial damage-contact model

A two-scale, delay-damage cohesive model for cracking and contact problems is employed herein to capture dynamic fracturing in rocks where as a highly heterogeneous material, crack nucleation and growth from weak points is the primary mechanism of fracture. As shown in Figure 4, a macroscopic damage parameter D describes the area fraction of debonded interface in the mesoscopic neighborhood $N(x)$ of a point x on a cohesive interface. The damage parameter vanishes where the interface is undamaged, and $D = 1$ where the interface is, locally, completely damaged, *i.e.*, debonded. A time-delay equation governs the macroscopic evolution of D in response to the local stress state, while the standard Riemann solution for a material interface holds in fully bonded mesoscopic zones and the contact model developed in the previous chapter governs the interfacial response in mesoscopic, debonded regions. Rather than refer to a traction-separation relation, we use a simple averaging of the mesoscopic model to determine the macroscopic cohesive response.

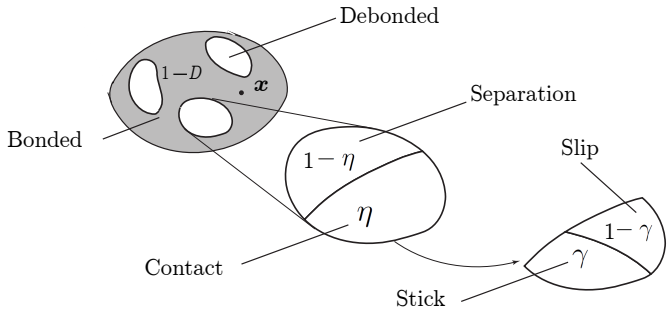

Figure 4: Schematic of contact-mode hierarchy and corresponding fractions

Figure 5 illustrates an active, fully developed fracture process zone in the employed interfacial-damage cohesive model. The cohesive surface tip (CST) is the leading edge of the cohesive process zone where interfacial damage begins to accumulate from $D = 0$ until complete damage, $D = 1$, is attained at the trailing edge of the process zone.

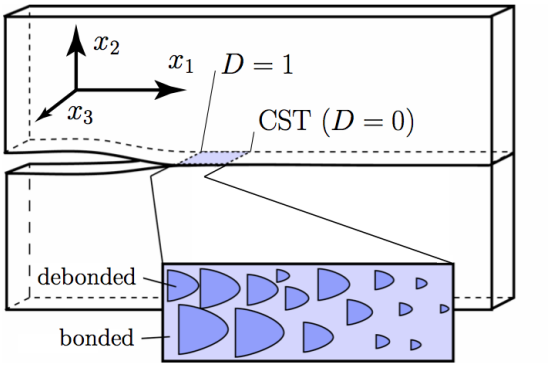

Figure 5: Cohesive process zone and the crack propagation mechanism

The crack propagation criterion is tested every time a patch is pitched over an active CST vertex, such as V in Figure 3. Vertex V may be the tip of an advancing crack as illustrated in the figure or be a newly nucleated CST. The weighted averages of D and $(1 - D)$ is used to define the macroscopic target Riemann stress at each point as:

$$\boldsymbol{\sigma}^* = (1 - D)\ \boldsymbol{\sigma}_B^* + D\ \boldsymbol{\sigma}_D^* \tag{3}$$

where $\boldsymbol{\sigma}_B^*$ and $\boldsymbol{\sigma}_D^*$ are the bonded and debonded stress vectors, respectively. Any point on an interface can take three different statuses of contact in debonded mode (*i.e.*, separation, contact–stick or contact–slip). Figure 4 shows the hierarchy of mesoscale contact modes in the neighborhood of a macroscopic point in the contact set. At the first level of subdivision, the debonded part of the interface is partitioned into regions that are either in contact mode or in separation mode, with respective area fractions $\eta \in [0, 1]$ and $1-\eta$, relative to the debonded area. The connectivities of these regions may be arbitrarily complex. However, the connectivities do not influence the macroscopic target stress and velocity values generated by our simple averaging scheme, so we are not concerned with them here. However, we do treat η as a continuous variable to support regularization of the separation–contact transition. The second level of subdivision partitions the contact region into contact–stick and contact–slip regions, with respective area fractions $\gamma \in \{0, 1\}$ and $1 - \gamma$ relative to the area of the contact region. We treat γ as a binary variable because we have no need to regularize the stick–slip transition. See [18] for identifying the mesoscale parameters, η and γ.

Rapid contact transitions and sharp moving fronts make dynamic contact modeling very challenging. Numerical solutions typically suffer from nonphysical oscillations or under/overshoots at these transitions. Artificial diffusion, although may reduce these features, excessively smoothens the solution in general. The set of contact property solutions employed preserve the characteristic structure of elastodynamics and enable us to capture these sharp transitions with almost no numerical artifacts. In addition, these solutions were integrated with the interfacial damage model to study combined contact and fracture problems and smooth transitions of various contact modes occur. For example, the direction of the slip transition is ambiguous at stick-slip transition and it calls for regularization in almost all numerical methods. It has been demonstrated that this transition is in fact continuous and no regularization is required while this set of solutions is used. The only separation to contact transition physically induces shocks and a regularization scheme with tunable maximum penetration was implemented to treat this issue. Details of contact model's features and formulation have been provided in [18]

3 NUMERICAL APPLICATIONS

In the stimulation techniques in which static loadings are applied, the cracks generated is proportional to the energy transferred to the volume of material being broken. However, dynamic loadings apply a large amount of energy to a small volume of material. In this situation, a large area of cracks will be created. As the loading wave spreads inside the material, it will create fragmentations, thereby connecting the natural and induced fractures. Utilizing explosives as a stimulation technique in tight formations to increase production is a very old technique, which is also widely employed in mining and known as well shooting. Besides, the burn of a propellant in a well is a rapid oxidation reaction causing the release of gaseous energy. Figure 6 shows three typical pressure-time profiles of explosive, propellant and the conventional hydraulic fracturing events in which the loading rates differ in the scales noted in the figure. As observed, a propellant event is therefore *intermediate* in comparison to the other two methods in its energy release rate.

Two loading rates are considered herein for the application part to demonstrate the performance of our dynamic approach for tight formation stimulations. As the first problem, a well is pressurized in a very high loading rate to indicate an explosive loading. In the next examination, we simulate a perforated wellbore subjected to an intermediate loading rate. Therefore, the second problem followed in this section is devoted to propellant fracturing from the oriented perforations.

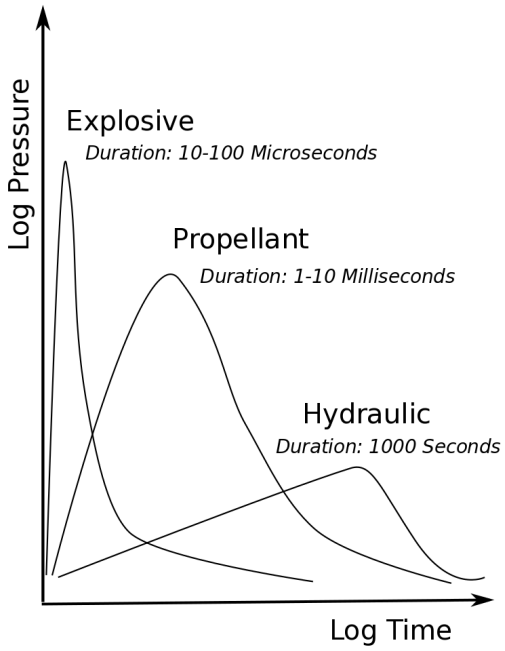

Figure 6: Pressure-time profiles of three stimulation approaches

The fluid pressure along fracture faces, specifically near the wellbore can be treated as a nearly constant due to the high *in-situ* stresses acting as effective confining pressures in the deep reservoirs and the low fluid viscosity. Utilizing analytical solutions for this problem, references [11, 22] showed that considering this behavior is reasonable. Allowing that, it is also practical to deduce that the fluid and fracture fronts occur simultaneously and are coincident, which means the fluid lag is negligible. It should be noted that the size of the fluid lag is inversely proportional to σ_0^3, in which σ_0 is the far field confining stress [23]. In the following, the maximum and minimum compressive stresses are denoted as σ_H and σ_h, respectively.

3.1 Explosive fracturing

A pressurized wellbore in a domain, which is subjected to far field confining stresses as bi-axial tractions, is considered in the following examination. The problem sketch is illustrated in Figure 7. The diameter of the wellbore is 0.30 m and is subjected to the confining *in-situ* stresses as $\sigma_h = \sigma_H = 3.6375$ MPa. The material properties are: Young's modulus $E = 20$ GPa, Poisson's ratio $v = 0.2$ and the tensile strength of 2 MPa. The fluid pressure is assumed to increase in time as a dynamic loading from a stabilizing constant pressure being applied as a static load. A maximum pressure of 38.8 MPa based on the profile shown in Figure 6 with the total duration of 0.4 ms is applied to the sidewalls of the well. Since, there is no explicit nucleation point for fractures to be initiated from, the probabilistic nucleation method discussed in the previous section is used here.

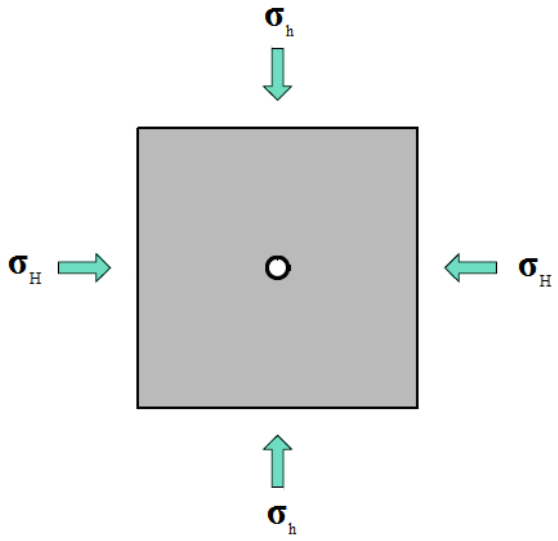

Figure 7: Problem sketch for the explosive fracturing application

Evolution of damage which is mostly in shear mode is shown in Figure 8. Furthermore, fracture visualizations of the solution are illustrated in Figure 9 for the corresponding time frames shown in the damage evolution figures. When the explosive is detonated in practice, an extremely high and compressive pressure pulse, or shock wave is generated, which far exceeds the tensile strength of the formation rock. The high pressures of the detonation cause the rock to yield and compact. After the stress wave passes, the rock unloads elastically, leaving an enlarged, deformed wellbore, a zone of compacted rock and a region of greater compressive stress. Herein, the cracks occurring are almost all in shear damage mode. As reported from experiments in practice, this crushed region may reduce permeability and productivity around the wellbore.

3.2 Propellant fracturing

Before performing hydraulic fracturing in practice, wellbores usually are cased and then perforated to isolate the well from undesirable regions and to consider some operational considerations in the field along with stability concerns. These perforations generated during the process of a well completion play the role of a transmission channel between the wellbore and the reservoir. In fact, a perforation may serve as an initial fracture to help with crack nucleation and

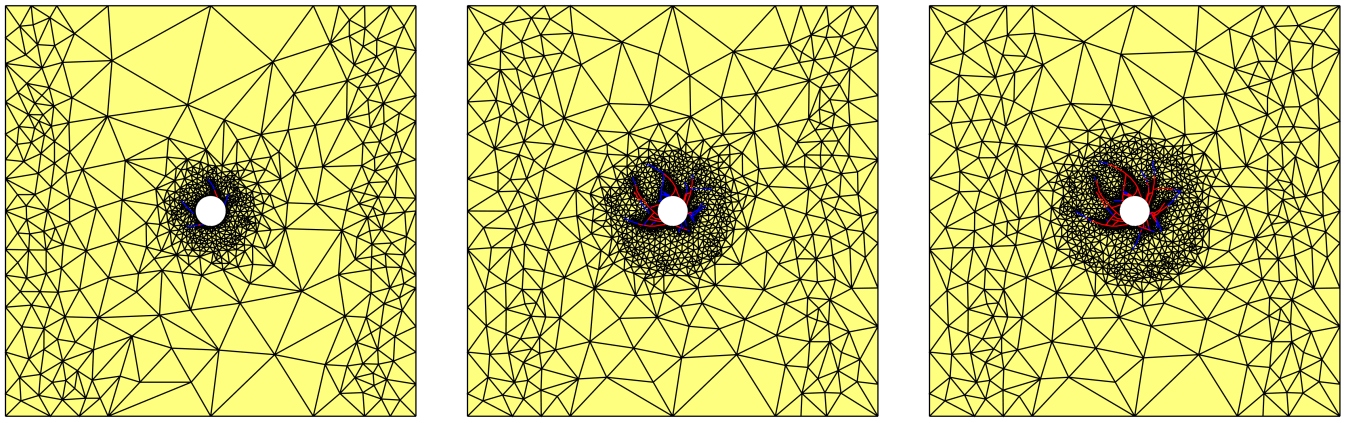

(a) time ≈ 0.033 ms (b) time ≈ 0.062 ms (c) time ≈ 0.077 ms

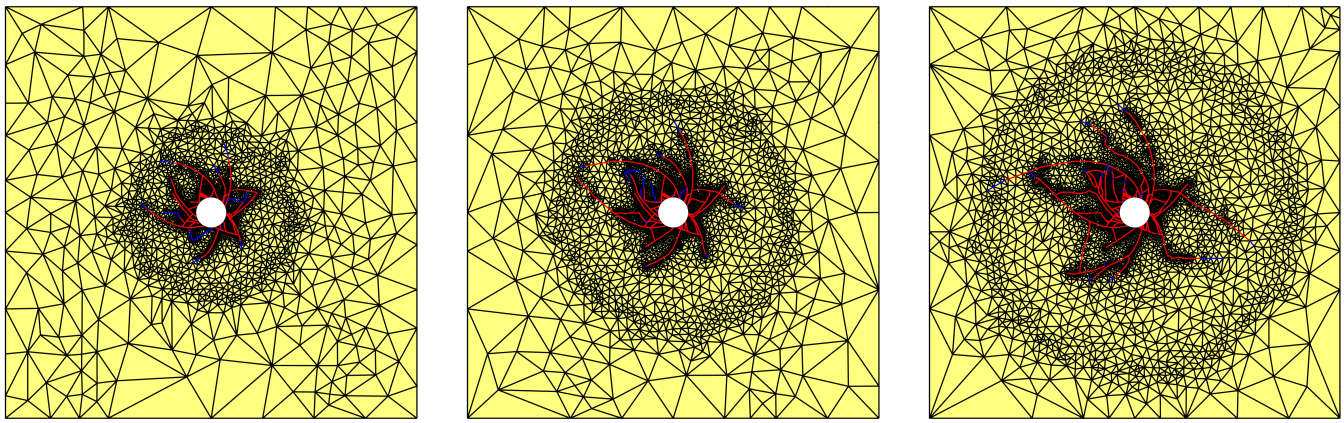

(d) time ≈ 0.098 ms (e) time ≈ 0.148 ms (f) time ≈ 0.207 ms

Figure 8: Evolution of damage in solution of a well stimulation by explosive fracturing technique

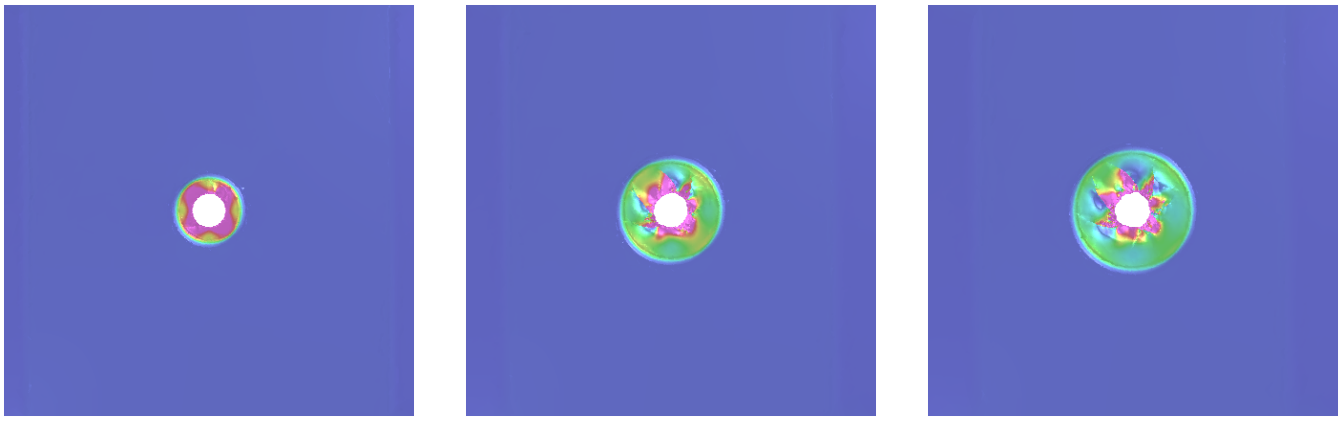

(a) time ≈ 0.033 ms (b) time ≈ 0.062 ms (c) time ≈ 0.077 ms

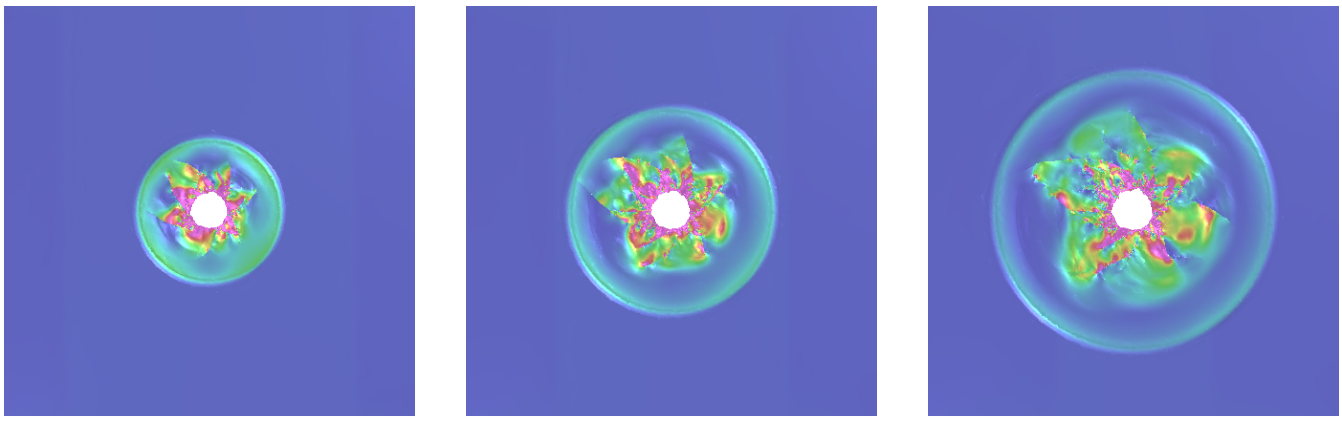

(d) time ≈ 0.098 ms (e) time ≈ 0.148 ms (f) time ≈ 0.207 ms

Figure 9: Visualization of fracture evolution in solution of a well stimulation by explosive fracturing technique

slightly force propagation direction to perform an efficient treatment. Therefore, perforations are important in the complex fracture geometries around wellbore. The success of stimulation treatment through perforations depends on several parameters including its length, diameter along with permeability of the rock around the perforation. The enhanced permeability of the rock around the wellbore controls recovery flow through a perforation. By shortly reviewing effective parameters, which are important for a perforation design, the function of perforation in hydraulic fracturing is discussed in the following. Perforation phasing, which is the angle between the two successive perforations, is another important parameter affecting production rate and needs to be carefully assessed at its design stage. Common perforation phasing angles are 60^o, 90^o, 120^o and 180^o.

Herein, as sketched in Figure 10 one application with phasing angles of 90^o is considered. All parameters are same as the previous example, except the rate and duration of the loading. In this application, a maximum pressure of 19.4 MPa during a total time of 2 ms is applied to the sidewalls of the well and inside the perforation surfaces. Unlike the explosive stimulation example in which there was not any nucleation point to initiate cracking, here there are four crack tips and we can expect that all fracturing start from these tips. The results of damage evolution and fracture opening visualizations for several time frames have been plotted in Figures 11 and 12, respectively. The damages occurred in this simulation are mostly in tensile mode where we expect to have fracture opening in the visualizations of the solution shown in Figure 12.

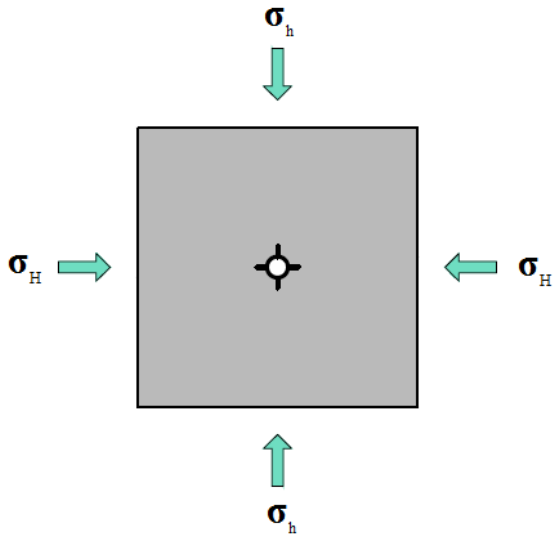

Figure 10: Problem sketch for the propellant fracturing application in a well with four perforations

As observed, a propellant stimulation rapidly exceeds the fracture pressure of the rock and maintain the pressure but do not crush the rock as we noticed in the explosive stimulation application. As a result, propellants pressurize and break down all perforations along a significant fracturing and penetrate farther in comparison with explosive fracturing. The advantages of propellant stimulation approach over the conventional hydraulic fracturing is that multiple fractures are created, consequently the entire considered zone is stimulated. Besides, there is no need to inject fluids, which makes it a better choice to protect the environment. Of course, it is not a complete replacement for hydraulic fracturing and when hydraulic fracturing is not practical economically, it can be an initial treatment prior to fracking.

4 CONCLUSIONS

One of the most important applications of hydraulic fracturing nowadays is to improve the recovery of unconventional hydrocarbon reservoirs. Having an appropriate fracture propagation model in rocks is a crucial issue for a hydraulic fracture design. Many approaches have been developed to efficiently perform crack growth simulations, which are mostly based on either efficient remeshing techniques or the XFEM/GFEM employing fixed meshes, but these are mainly limited to the linear elastic fracture mechanics (LEFM) framework. In this paper, an interfacial damage model implemented in a Spacetime Discontinuous Galerkin (SDG) framework is utilized to simulate nucleation and then propagation of hydraulically induced fractures in an oil reservoir. The SDG method offers many advantages over conventional and extended/generalized finite element methods including dynamic adaptive meshing, interface tracking, and element-wise conservation. To facilitate crack propagation in any arbitrary direction we use the SDG's powerful adaptive meshing capabilities to align cracks with inter-element boundaries; Unlike the XFEM methods no special discontinuity functions are required.

Hydraulic fracturing has been widely employed for well stimulation in the last five decades. Different techniques, equipment, fracturing fluids and proppants have been utilized in practice to optimize the fracturing process. However, it has some disadvantages including a lack of control over the direction of fracture propagation, the high treatment cost along with some challenging environmental issues. Dynamic stimulation techniques generating multiple fractures in a wellbore to enhance gas recovery

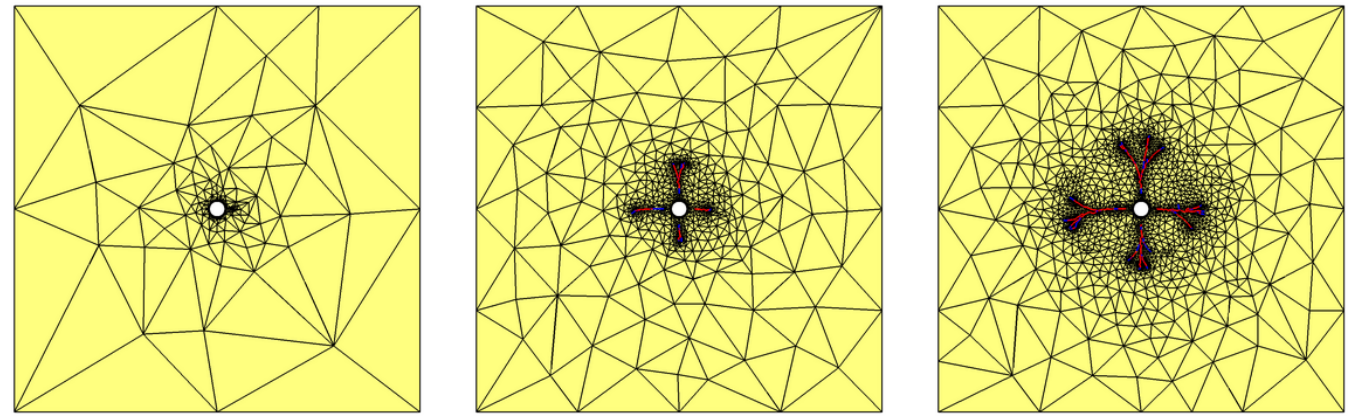

(a) time ≈ 0.102 ms (b) time ≈ 0.510 ms (c) time ≈ 0.715 ms

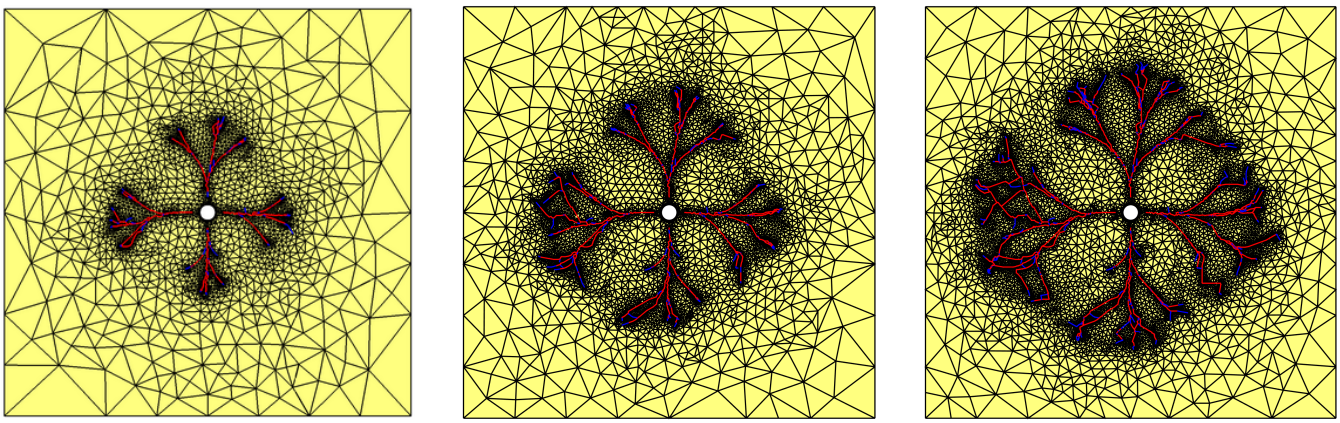

(d) time ≈ 0.863 ms (e) time ≈ 1.037 ms (f) time ≈ 1.165 ms

Figure 11: Evolution of damage in solution of a well stimulation by propellant fracturing technique

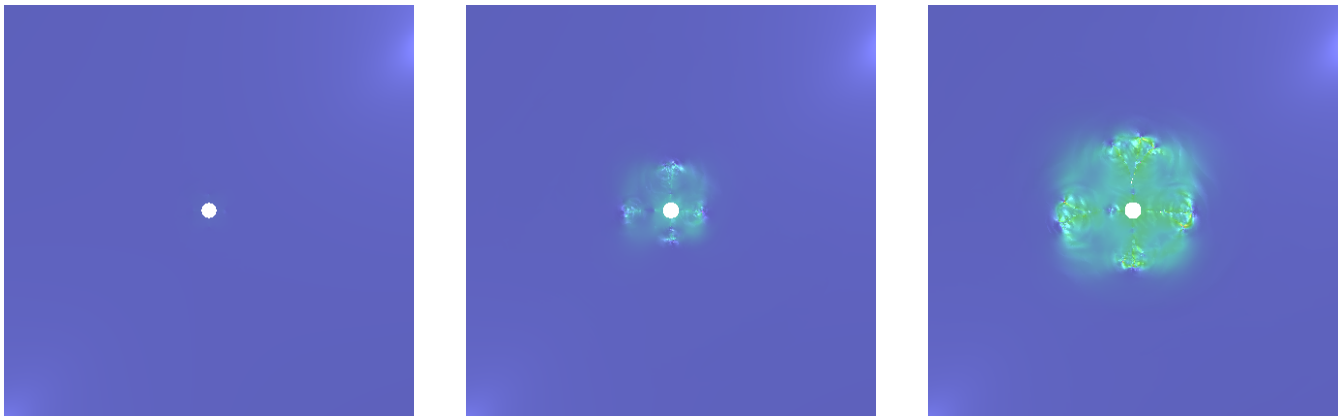

(a) time ≈ 0.102 ms (b) time ≈ 0.510 ms (c) time ≈ 0.715 ms

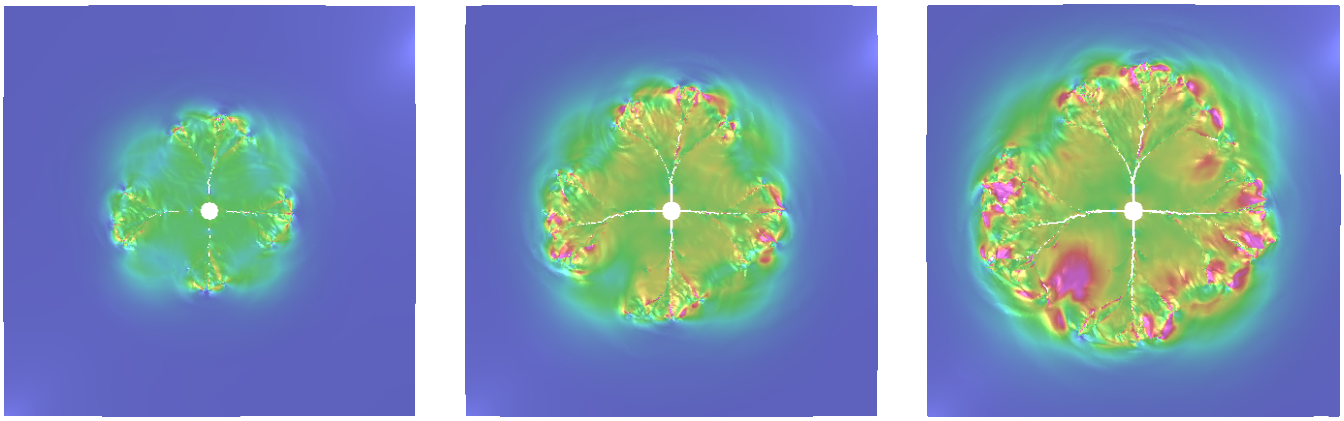

(d) time ≈ 0.863 ms (e) time ≈ 1.037 ms (f) time ≈ 1.165 ms

Figure 12: Visualization of fracture evolution in solution of a well stimulation by propellant fracturing technique

are nowadays attracting more attention in oil industry. Producing multiple fractures seems to be more promising in naturally fractured reservoirs, since it is an effective way for connecting a pre-existing fracture network to a wellbore. Applying high rate loadings by explosives and propellants are the two common methods for dynamic stimulation of a well.

The technique using explosives, which is also called well shooting in the literature, has been found to have damaging effects on the well since it causes crushing and plastic flow near the borehole which can possibly result in a severely locked formation rather than the multiple fracture pattern desired for enhancing permeability. Whereas the pressure loading rate is too slow, a single extensive hydraulic fracture is produced. On the other hand, dynamic stimulations through propellants utilizing intermediate loading rate in comparison with slow rates in hydraulic fracturing and fast rates in explosive fracturing can generate multiple fractures without excessive crushing or residual damage around the borehole.

Although hydraulic fracturing has been employed for several decades in oil industry, a thorough understanding of the interaction between induced hydraulic fractures and pre-existing natural fractures is still challenging. Our approach is also applicable to hydraulic fracturing where an induced major crack propagates and intersects natural fractures which in turn are hydraulically loaded and extended to intersect other fissures resulting in a complicated fracture network. Furthermore, incorporation of macro-micro crack interactions can explain discrepancies for tracking efficiency between real productivity and computational estimations. The future work focuses on utilizing the developed interfacial damage model in capturing the interactions between hydraulically induced fractures and natural fractures.

Water usage is reduced or completely eliminated in the stimulation methods using dynamic loadings, however they usually suffer from some potential disadvantages including higher costs, riskier due to using a dangerous substance and limited possibility to operate at depth. Although these new techniques could help address the environmental concerns, the hydraulic fracturing is still the preferred approach by the oil industry. Therefore, a combination of these techniques might be more effective. The main advantage of propellant fracturing is to create multiple cracks and consequently prepare the well for an effective hydraulic fracturing with much lower cost as a re-fracturing solution.

REFERENCES

[1] Huang, B., C. Liu, J. Fu, and H. Guan (2011) Hydraulic fracturing after water pressure control blasting for increased fracturing. *International Journal of Rock Mechanics and Mining Sciences*, **48**, 976–983.

[2] Shojaei, A., A. Dahi-Taleghani, and G. Li (2014) A continuum damage failure model for hydraulic fracturing of porous rocks. *International Journal of Plasticity*, **59**, 199–212.

[3] Busetti, S., K. Mish, P. Hennings, and Z. Reches (2012) Damage and plastic deformation of reservoir rocks: Part 2. propagation of a hydraulic fracture. *AAPG Bulletin*, **96**, 1711–1732.

[4] Galindo Torres, S.A. and J.D. Muñoz Castaño (2007) Simulation of the hydraulic fracture process in two dimensions using a discrete element method. *Phys. Rev. E*, **75**, 066109.

[5] Zhao, Q., A. Lisjak, O. Mahabadi, Q. Liu, and G. Grasselli (2014) Numerical simulation of hydraulic fracturing and associated microseismicity using finite-discrete element method. *Journal of Rock Mechanics and Geotechnical Engineering*, **6**, 574–581.

[6] Dahi-Taleghani, A. and J.E. Olson (2011) Numerical modeling of multistranded-hydraulic-fracture propagation: Accounting for the interaction between induced and natural fractures. *SPE Journal*, **16**, 575–581.

[7] Chen, Z. (2013) An abaqus implementation of the xfem for hydraulic fracture problems. *International Society for Rock Mechanics*.

[8] Mohammadnejad, T. and A.R. Khoei (2013) An extended finite element method for hydraulic fracture propagation in deformable porous media with the cohesive crack model. *Finite Elements in Analysis and Design*, **73**, 77–95.

[9] Gupta, P. and C.A. Duarte (2014) Simulation of non-planar three-dimensional hydraulic fracture propagation. *International Journal for Numerical and Analytical Methods in Geomechanics*, **38**, 1397–1430.

[10] Gupta, P. and C. A. Duarte (2015) Coupled formulation and algorithms for the simulation of non-planar three-dimensional hydraulic fractures

using the generalized finite element method. *International Journal for Numerical and Analytical Methods in Geomechanics*, pp. n/a–n/a.

[11] Gordeliy, E. and A. Peirce (2013) Implicit level set schemes for modeling hydraulic fractures using the {XFEM}. *Computer Methods in Applied Mechanics and Engineering*, **266**, 125–143.

[12] Bazant, Z. P. and F. C. Caner (2014) Impact comminution of solids due to local kinetic energy of high shear strain rate: I. continuum theory and turbulence analogy. *Journal of the Mechanics and Physics of Solids*, **64**, 223–235.

[13] Chen, Wen, Olivier Maurel, Christian La Borderie, Thierry Reess, Antoine De Ferron, Mohammed Matallah, Gilles Pijaudier-Cabot, Antoine Jacques, and Frank Rey-Bethbeder (2014) Experimental and numerical study of shock wave propagation in water generated by pulsed arc electrohydraulic discharges. *Heat and Mass Transfer*, **50**, 673–684.

[14] Moes, N., J. Dolbow, and T. Belytschko (1999) A finite element method for crack growth without remeshing. *International Journal for Numerical Methods in Engineering*, **46**, 131–150.

[15] Grasselli, Giovanni, Andrea Lisjak, Omid K. Mahabadi, and Bryan S.A. Tatone (2015) Influence of pre-existing discontinuities and bedding planes on hydraulic fracturing initiation. *European Journal of Environmental and Civil Engineering*, **19**, 580–597.

[16] Omidi, O., R. Abedi, and S. Enayatpour (2015) An adaptive meshing approach to capture hydraulic fracturing. *In Proceedings of the 49th US Rock Mechanics/Geomechanics Symposium*, pp. ARMA 15–572.

[17] Abedi, Reza (2010) *Spacetime damage-based cohesive model for elastodynamic fracture with dynamic contact*. Ph.D. thesis, Department of Theoretical and Applied Mechanics, University of Illinois at Urbana–Champaign.

[18] Abedi, Reza and Robert B. Haber (2014) Riemann solutions and spacetime discontinuous Galerkin method for linear elastodynamic contact. *Computer Methods in Applied Mechanics and Engineering*, **270**, 150 – 177.

[19] Abedi, Reza, Robert B. Haber, and Boris Petracovici (2006) A spacetime discontinuous Galerkin method for elastodynamics with element-level balance of linear momentum. *Computer Methods in Applied Mechanics and Engineering*, **195**, 3247–3273.

[20] Abedi, R., R. B. Haber, S. Thite, and J. Erickson (2006) An h–adaptive spacetime–discontinuous Galerkin method for linearized elastodynamics. *Revue Européenne de Mécanique Numérique (European Journal of Computational Mechanics)*, **15**, 619–642.

[21] Abedi, Reza, Morgan A. Hawker, Robert B. Haber, and Karel Matouš (2009) An adaptive spacetime discontinuous Galerkin method for cohesive models of elastodynamic fracture. *International Journal for Numerical Methods in Engineering*, **1**, 1–42.

[22] Detournay, E. (2004) Propagation regimes of fluid-driven fractures in impermeable rocks. *International Journal of Geomechanics*, **4**, 35–45.

[23] Lecampion, B. and E. Detournay (2007) An implicit algorithm for the propagation of a hydraulic fracture with a fluid lag. *Computer Methods in Applied Mechanics and Engineering*, **196**, 4863–4880.